CGU HS Committee on River Ice Processes and the Environment
18th Workshop on the Hydraulics of Ice Covered Rivers
Quebec City, QC, Canada, August 18-20, 2015

An Experimental Investigation of Turbulent Flow Characteristics Beneath an Ice Jam

Hoda Pahlavan[1a], Shawn P. Clark[1b], Ming Wang[2a], Jarrod Malenchak[2b]
[1]Department of Civil Engineering, University of Manitoba
15 Gillson Street, Winnipeg, Manitoba R3T 5V6
[a]pahlavah@myumanitoba.ca
[b]Shawn.Clark@umanitoba.ca

[2]Manitoba Hydro, 360 Portage Ave, Winnipeg, Manitoba R3C 0G8
[a]swang@hydro.mb.ca
[b]JMalenchak@hydro.mb.ca

Extreme flood events created by river ice jams cause major damage to infrastructure and riverside communities. In Canada, damage due to ice jams has created annual damage in the millions. Safety concerns prevent detailed flow measurement beneath an ice jam in the field, and there is a paucity of data in the literature regarding flow characteristics beneath a simulated ice jam; which contributes to our lack of understanding of ice jams in general. To help bridge this gap, this research aims to quantify the turbulent flow characteristics beneath a simulated smooth ice jam. Measurements were taken at various streamwise locations beneath the simulated jam using an acoustic Doppler velocimeter. The measurements showed the streamwise flow velocity and turbulence intensity varied depending on the location under the jam. The maximum velocity was observed near the toe of the jam. In addition, the peak value of the turbulence intensity also occurred near the toe of the jam close to the ice cover. It is anticipated that these results and future experimental work will improve our fundamental understanding of flow beneath an ice jam, and may be used for validation of subsequent ice jam numerical models.

1. Introduction

In northern countries, river ice jams are an important issue due to the potential for economic, environmental, and ecological damage (Beltaos, 2008). Canada in particular has experienced extreme flood events caused by river ice jams (Beltaos, 1995; Beltaos and Burrell, 2002). The Dauphin River, the Nelson River, and mouth of the Red River in Manitoba are examples of rivers that are prone to such events. A number of research projects have been conducted to better understand river ice jam processes. These attempts will help to prevent or reduce the impacts of ice jams on hydroelectric power generation, transportation, and other facilities close to rivers.

In general, ice jams form when moving ice pieces become arrested at a particular location such as upstream of a large intact ice sheet, artificial obstruction (e.g., bridge piers), river bends, and natural constrictions including those caused by border ice formation. There are different types of ice jams; however, this study is focused on an equilibrium ice jam as discussed in Beltaos, 2008 and 1995. An equilibrium ice jam forms when the upstream ice supply is steady and continuous for a long period of time. This jam is comprised of three regions: an upstream transition, an equilibrium reach, and a downstream transition as shown in Figure 1 (Beltaos, 2008).

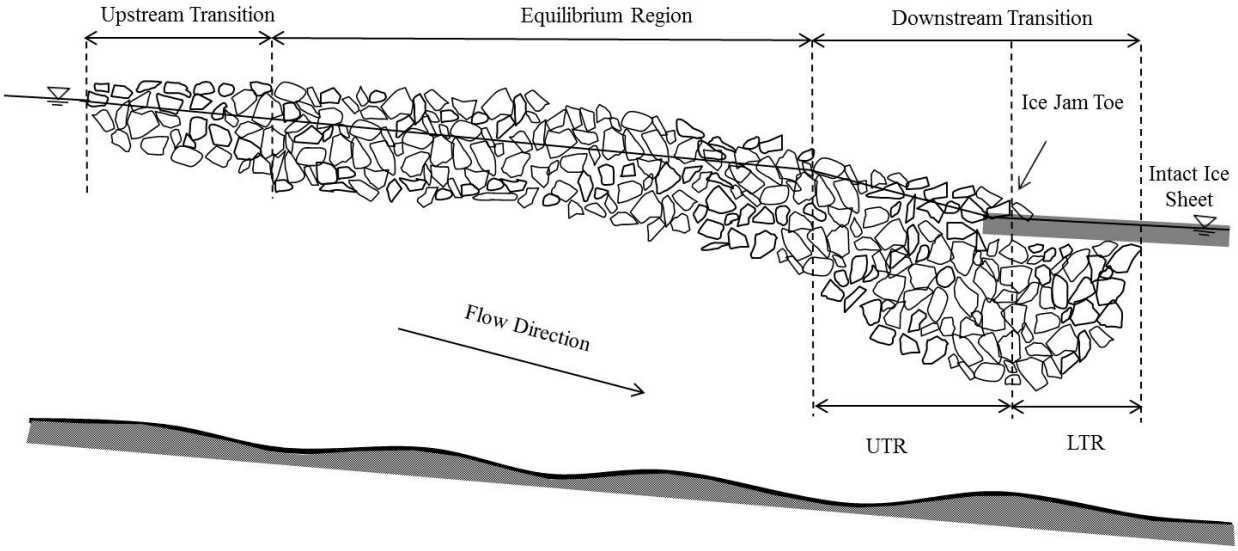

Figure 1. Schematic side view of an equilibrium ice jam (adapted from Beltaos, 2008)

In the upstream transition, incoming ice pieces are added to the ice jam, thereby increasing its total length. The jam thickness in the upstream transition region increases with downstream distance. In the equilibrium region, incoming ice pieces increase the jam length rather than the jam thickness due to a balance in resisting and driving forces on the ice cover; hence, the jam thickness remains constant in this region. The water surface and channel bed slope are equal in this region. In the downstream transition, the jam thickness increases depending on various factors such as channel slope, flow velocity, incoming ice volume, channel bed morphology, roughness under the intact ice cover, etc. In this region, the jam thickness grows until it meets with the lower water depth at the toe of the jam. This region consists of two parts: an upper toe region (UTR) and a lower toe region (LTR). Unlike the equilibrium region, the water surface slope is steeper than the channel bed slope in the downstream transition region.

In a river ice jam, flow features under an ice jam are significantly different to that of open rivers. Safety concerns, thickness of the ice cover, and technology limitations prevent detailed flow measurements beneath an ice jam in the field; therefore, there is a scarcity of data in the literature regarding flow characteristics beneath ice jams. The motivation of this research was to contribute to the fundamental understanding of the flow characteristics beneath an ice jam. To bridge the knowledge gap, the objective of this study was to measure water velocity and quantify the turbulent flow statistics at various streamwise locations beneath a simulated ice jam. Moreover, the research provides data to validate future numerical models of ice jams.

2. Literature Review

Several theoretical and experimental studies have been conducted to investigate ice jam formation and development (Pariset and Hauser, 1961; Zulfet and Ettema, 1997; Hicks and Bonneville, 1998). A set of comprehensive studies about the freeze-up and break-up of ice jams were accomplished by Beltoas in 1985 and 2008. Field investigations of river ice jams have been undertaken across Canada (Beltaos and Moody, 1986; Beltaos et. al., 1996; Prowse, 1986; Kowalczyk and Hicks, 2003; She et. al., 2009). In addition, several numerical models have been developed to predict the formation of river ice jams (Beltaos, 1993; Shen, 2002; Carson et. al., 2011). Despite the considerable amount of knowledge gained by these studies, flow features underneath ice jams are still not fully understood.

Yamaguchi and Hirayama (1990) conducted field measurements over three winters in several rivers in Hokkaido, Japan, to investigate the velocity profile under ice covers with various roughnesses. They utilized a Pitot tube and a propeller-type current meter for their measurements in shallow and deep depths, respectively. They showed that the average velocity in the bed-affected area (distance between the channel bed and maximum velocity location) was less than the ice-affected area (distance between the maximum velocity location and under-side of the ice cover). They also indicated that although the velocity distribution in both the bed- and ice-affected areas followed a logarithmic distribution, the calculated maximum velocity using the logarithmic distribution was slightly larger than the measured one.

Healy et. al. (2002) carried out an experimental study to examine the velocity distribution under an ice cover. They used a flexible rubber mat with a rough underside as a simulated floating ice cover and applied Prandlt tubes for the velocity measurements. They concluded that the velocity profiles under the cover were generally the same in both steady and unsteady flow conditions, with small differences observed between the steady and highly unsteady flow conditions. Moreover, they found the two-point measurement method was applicable to estimate average velocity for steady and unsteady flow conditions.

Flow velocity and turbulence features beneath simulated ice covers with various roughnesses over a sand bed were examined by Parthasarathy and Muste (1994). They simulated ice covers using plywood sheets that created both smooth and rough cover conditions. The first was smoothened using paint, while second and third covers were made rough by attaching a wire mesh and wooden strips. They used a laser Doppler velocimeter (LDV) to measure flow velocities. They found that the streamwise velocity for the open channel and ice-covered conditions followed the logarithmic law. They also found that the streamwise and vertical turbulence intensities agreed with equations given by Nezu and Rodi (1986), for the ice- and bed-affected areas.

Robert and Tran (2012) performed experiments to quantify turbulent flow features under open channel conditions as well as a rough simulated ice cover over a gravel bed. They used an acoustic Doppler velocimeter (ADV) to measure streamwise water velocity and turbulence intensity along vertical profiles at several streamwise locations. The results suggested that the presence of the additional rough boundary at the surface did in fact influence the turbulent flow quantities; however, their measurements were limited to the bottom 70% of the flow depth due to equipment constraints. Direct measurements near the underside of the simulated rough cover were therefore not obtained.

Wubben (1988) conducted experiments to examine scour patterns beneath an ice jam on a movable sand bed. He modeled the upstream transition and equilibrium region of the ice jam using a floating plywood box of uniform thickness with a sloped leading edge. The jam was located behind a simulated intact ice cover using Styrofoam. However, the downstream transition of the jam was not completely modeled. The streamwise flow velocity profiles at different locations beneath the jam were shown; however, details were limited. The results demonstrated that scour was a function of the jam thickness and that the maximum scour potential was located at the thickest portion of the jam.

3. Methodology

The experiments in this study were conducted in a fixed slope (0.25%) rectangular flume made of high density overlay (HDO) plywood (14 m long, 1.22 m wide, 0.6 m deep) in the Hydraulics Research & Testing Facility at the University of Manitoba (Figure 2). A flow straightener consisting of several rows of PVC pipes (0.14 m diameter, 0.25 m long) surrounded by two wire mesh screens was located in the large upstream head tank (3.68 × 2.43 m) to condition the flow. Water level in the flume was manually controlled by a gate acting as a weir at the downstream end of the flume. Two point gauges, one in the head tank and another at the downstream end of the flume were used to monitor the water level during the experiments. The water surface profile throughout the flume was measured using pressure taps connected to a manometer board.

A solid ice jam was constructed from HDO plywood sheets (2.44 m long, 1.22 m wide, 0.019 m thick). Starting at the upstream end two sheets of HDO were used to construct the equilibrium region (EQR) of the ice jam. Next, the downstream transition region of the jam consisted of two sections of HDO with lengths of 1.8 m and 0.64 m, set at a downward slope of 5º (UTR) and an upward slope of 14º (LTR), respectively. These slopes were selected as a compromise between the available field measurements and the physical limitations of the flume length and instrumentation. A downstream intact sheet (DIS) of ice was constructed using three sheets of HDO and the jam was fixed to the flume walls.

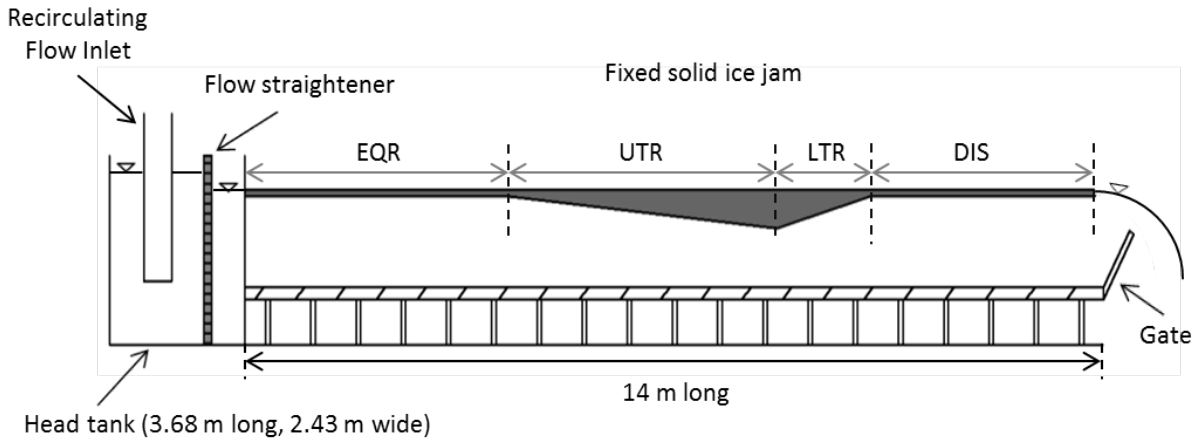

Figure 2. Experimental setup profile view (not to scale)

In this study, fifteen holes which were drilled along the centerline of the jam in order to facilitate water velocity measurement with an ADV, were selected. Three holes were placed in the EQR, six holes in the UTR, three holes in the LTR, and three holes in the DIS (Figure 3). When not in use for measurement access, the holes were plugged with HDO plywood flush to the underside of the ice cover.

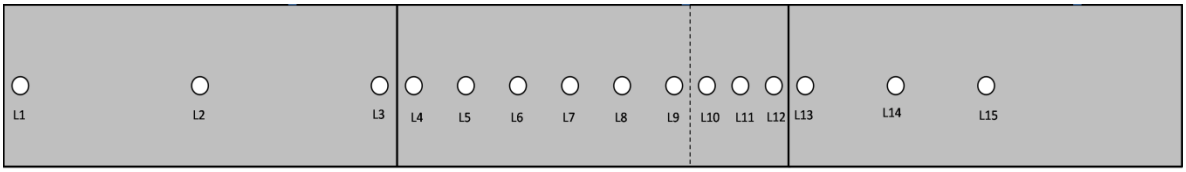

Figure 3. The simulated ice jam plan view with measured locations

An ultrasonic flow meter was used to measure the discharge. Three-dimensional water velocities were measured using a down-looking Nortek Vectrino profiler acoustic Doppler velocimeter. The ADV was mounted on a traversing mechanism; hence, it could be automatically moved in the vertical and lateral direction at sub-millimeter spatial resolution. The entire traversing mechanism and ADV had to be positioned manually along the streamwise direction. To measure the flow velocity profile near the boundaries (within 20% of the flow depth), measured points were spaced 8 mm apart from each other in the vertical direction. For the remainder of the water column, a distance of 10 mm was selected.

The ADV sampling volume was located 50 mm from the transmitter at the location where the receiver beams intersect. Since a down-looking ADV was used, and since the entire probe needed to be submerged in order to take measurements, the upper-most sampling location would be several centimeters beneath the ice cover. To facilitate measurements closer to the underside of the ice, once the ice cover elevation was fixed the entire ice cover was submerged by approximately 5 cm. Many wooden baffles covering the upper surface of the ice ensured that this submergence did not actually add to the channel conveyance. The benefit was that this allowed the ADV probe to be located above the simulated ice cover, while its sampling volume was located very near to the underside of the cover.

Initial convergence tests were conducted to determine the appropriate ADV sample size. Velocity measurements were collected at a frequency of 100 Hz near the flume bed and near the mid -depth for 30 minutes. Mean velocities and turbulence intensities were plotted against the number of samples to determine the suitable number of samples with an acceptable level of error. A total of

18,000 samples (3 min. duration) was found to have an uncertainty of ±0.15% for the streamwise mean velocity and ±1.1% for streamwise turbulence intensity. Although the Vectrino Profiler has the ability to measure 30 cells of 1 mm height simultaneously; only the central 7 cells were used in this study. The error associated with the ADV is ±0.5% of measured value ±1 mm/s (Nortek, 2013). Inherently, there are errors in the ADV's measurements due to instrument noise. Thus, a post-processing code in Matlab was utilized to eliminate or replace poor quality data to present more reliable and accurate results.

Prior to conducting the experiments with a simulated ice cover, an initial experiment under open channel conditions was undertaken. The flow became fully developed at a distance of 2.5 m downstream of the flume inlet. Measurements further down the flume confirmed that the flow was approximately symmetric across the flume centerline.

3.1. Experimental Conditions

The discharge was held constant at 92±2 l/s for all tests and the water level was maintained constant. The ADV and traversing mechanism were aligned using a level and square. The distance between each location and the flume inlet as well as the local flow depth at each location with the ice jam in place are shown in Table 1.

Table 1. Streamwise measurement locations and local flow depth

Location	Distance from the inlet (m)	Local flow depth, h (m)
L1	2.601	0.260
L2	3.660	0.260
L3	4.719	0.260
L4	5.041	0.246
L5	5.341	0.220
L6	5.641	0.194
L7	5.941	0.168
L8	6.241	0.142
L9	6.531	0.120
L10	6.853	0.145
L11	7.003	0.181
L12	7.153	0.218
L13	7.506	0.260
L14	8.150	0.260
L15	8.690	0.260

When determining the local flow depth for the experiment it was required that there should be enough room between the toe of the jam and the bed (h_{toe}) to measure velocity at a sufficient number of points to accurately capture velocity profiles. As such, the jam was placed in the flume

so that the h_{toe} was approximately 10 cm. Based on the requirements for the h_{toe} and selected UTR angle, the distance between the EQR and bed (h) was 26 cm. This configuration results in a bulk Froude number of 0.18 in the EQR.

4. Results and Discussion

4.1. Mean streamwise velocity profiles

The mean streamwise velocity (U) profiles under the simulated ice jam are presented in Figures 4 and 5, in which the velocity and distance from the bed were normalized by the local maximum velocity (U_{max}) and local flow depth (h), respectively. The velocity profiles in the EQR (L1, L2, and L3) are shown in Figure 4, where it is clear that the profiles for L2 and L3 are self-similar, demonstrating that the flow became fully developed by position L2. Of note is the fact that the roughness of the top and bottom are identical, and that the flow depth was nearly constant at 26 cm. The velocity profiles therefore show the expected parabolic shape with a maximum velocity at the mid-depth (Zulfet and Ettema, 1997).

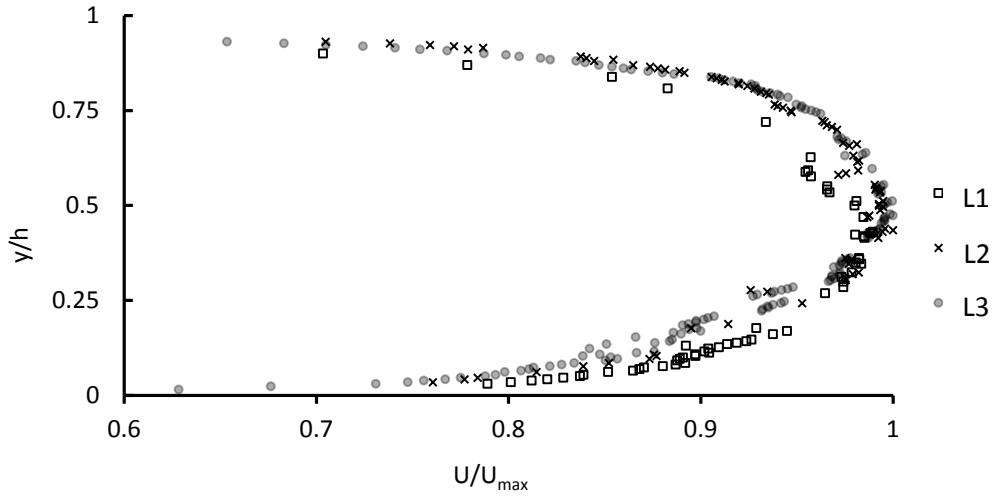

Figure 4. Dimensionless streamwise velocity profiles in the equilibrium region

In the UTR (Fig. 5(a) and (b)), as the flow contracted, the velocity close to the top boundary decreased. The down-sloping ice surface caused the streamlines to move more in the downwards direction, thereby decreasing the streamwise magnitude. In this part of the jam, the mean velocity increased compared to the EQR due to the flow area reduction and flow acceleration.
In the LTR (Fig. 5(c)), flow expanded because of the increasing cross sectional area. In this region the velocity profiles have a distinct S-shape with a zone of low velocity near the upper boundary. This was due to the effects of flow separation, and diminished as the flow developed and reattached to the upper boundary. As the water decelerated due to the expansion, the average velocity decreased.

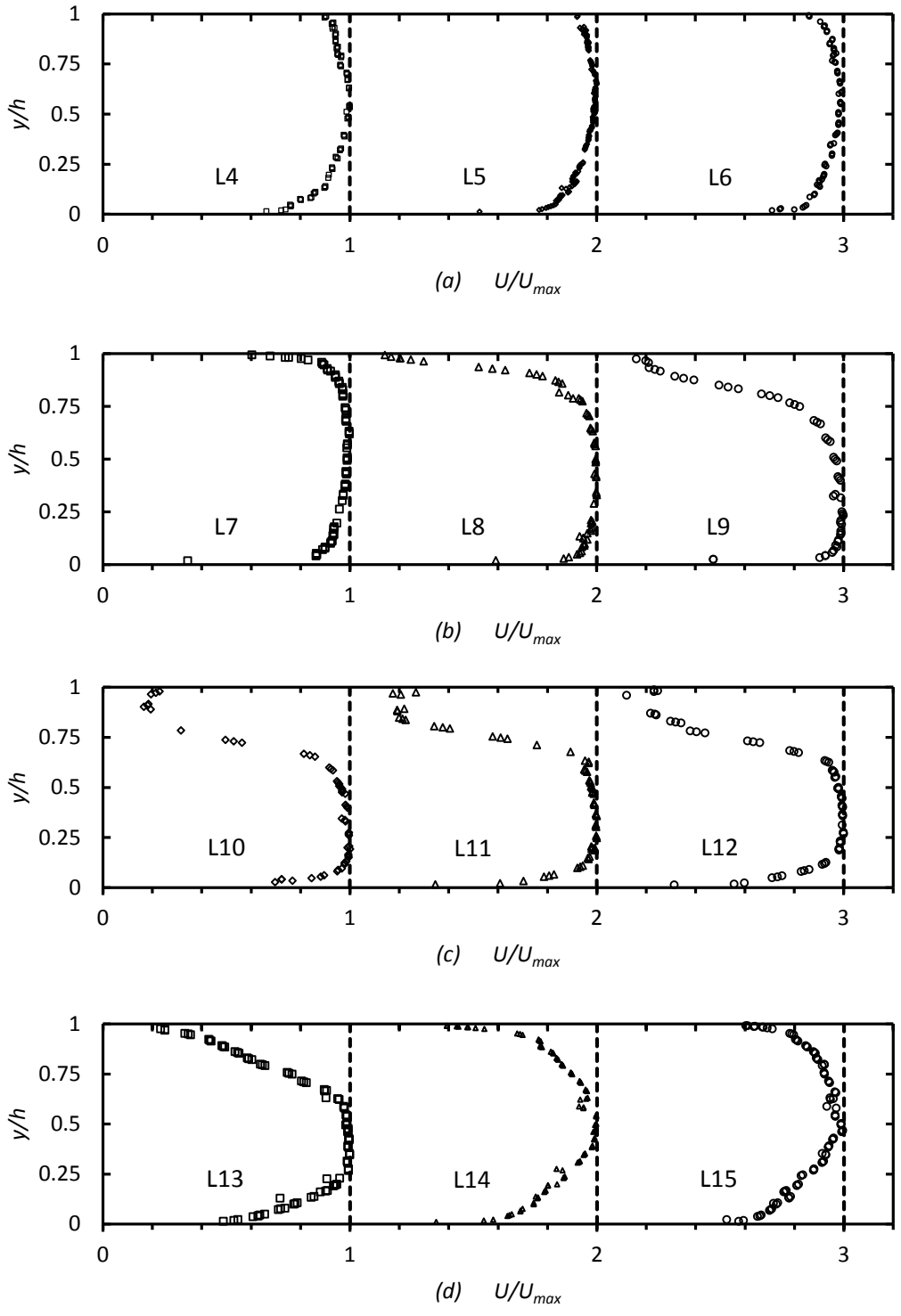

Figure 5. Dimensionless streamwise velocities in the (a) and (b) UTR, (c) LTR, (d) DIS

Under the DIS (Fig. 5(d)), the flow reattached to the upper boundary. The velocity profile in L13 differs from L14 while there is a small difference between the profile for L14 and L15.

In L13, the velocity gradient near the bed is higher than in L14, however, the velocity gradient in the top quarter of the flow depth of L13 is smaller than in L14, but becomes greater in the next lower quarter. Following L15, if the flow condition is the same as the EQR and the length of the downstream cover is sufficient, then the flow will tend to redevelop and return to that of the velocity distribution in the EQR. A summary of all streamwise velocity profiles beneath the ice jam at different locations is presented in Figure 6.

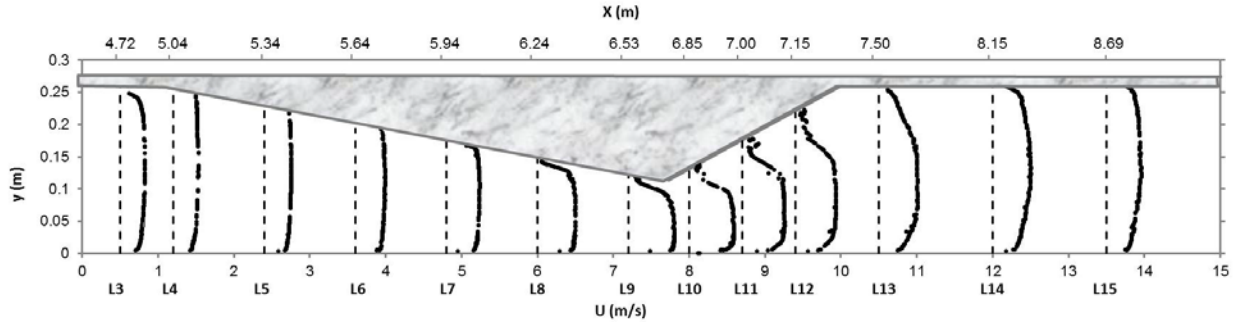

Figure 6. Streamwise velocities at different locations beneath the ice jam

4.2. Maximum velocity magnitude and location

The position of the local maximum streamwise velocity beneath the simulated ice jam is shown in Figure 7, along with the local mid-flow depth. It can be seen that the maximum velocity in the EQR occurred near the middle of the flow depth. When the uniform flow developed in the EQR reached the UTR, its momentum caused the location of maximum velocity to be above the mid flow depth. As the effects of the angled upstream boundary were felt by the flow, it begun to develop and the location of maximum velocity approached the mid flow depth. Near the toe of the jam (L8 and L9) the maximum velocity was below the mid flow depth and closest to the bed. The streamlines were contracted more in this area that causes the majority of the discharge to pass near the bed.

In the LTR, the maximum velocity began to move upward, but it remained below the mid flow depth. Similar to the UTR, the variation of the maximum velocity location in LTR was affected by the cross section area changes and the associated flow separation zone near the upper boundary. As the flow developed in this region, the zone of low streamwise velocity dimished, and the location of the maximum velocity moved upwards. In the DIS, the cross section area was constant and the flow separation zone disappeared, therefore the maximum velocity was observed again near the mid flow depth.

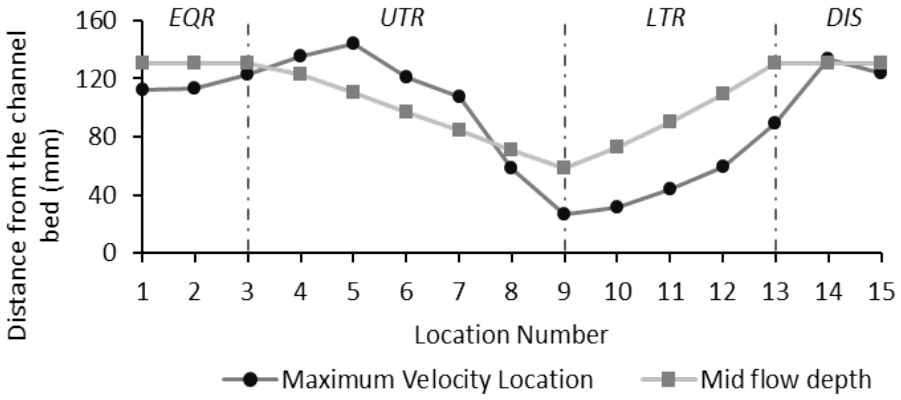

Figure 7. Vertical location of the maximum streamwise velocity under the ice jam

Figure 8 shows the magnitude of the maximum velocity at different locations beneath the jam. As expected, the maximum velocity increased through the UTR and the highest maximum velocity was observed near the toe of the jam (L9) at the measurement location with the smallest cross sectional area. Afterward, the value of the maximum velocity decreased until it stabilized at a constant value under the DIS. There is a slight difference between the maximum velocity at L1 and L15 since the flow at L15 was not yet fully developed. The results clearly show that near the toe of the jam the potential for bed scour would be greatest due to the largest maximum velocity being located nearest to the channel bed, causing a local bed shear stress that is approximately four times that of the EQR. These results correspond to the findings of Wuebben (1988) who observed scour potential near the toe of a jam was much larger than other locations under an ice jam.

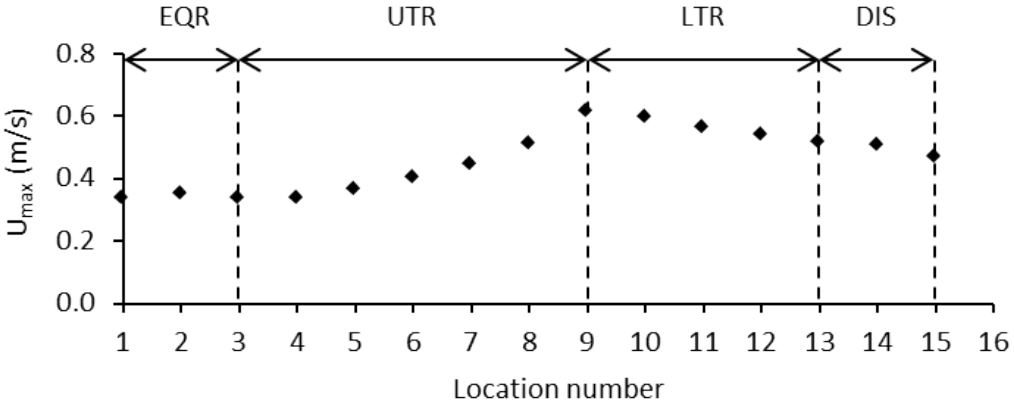

Figure 8. Magnitude of the maximum streamwise velocity under the ice jam

4.3. Streamwise Turbulence Intensity Profiles

The streamwise turbulence intensity (U_{rms}) results for each hole location are shown in Figure 9. The results from each location are normalized by the local maximum velocity. In the EQR (Fig.9(a)), the turbulence intensity is greatest near the upper boundary and has a minimum near the mid water depth. Conversely, in the open flow condition, turbulence intensity has its minimum value near the water surface. The results in the EQR are similar to the findings of Robert and Tran (2012) who presented streamwise turbulence intensity under a simulated rough cover and rough bed. In addition, the results agree with finding of Parthasarathy and Muste (1994) who presented

streamwise turbulence intensity under a simulated smooth cover and rough bed. The turbulence intensities from L2 and L3 have obtained self-similarity.

In the UTR (Fig. 9 (b) and (c)), the turbulence intensity in L4 was relatively constant. As flow developed downstream, the effect of the upper boundary on the turbulence intensity distribution increased. The peak value $(U_{rms}/U_{max})_{max}$ occurred close to the upper boundary and decreased rapidly away from the upper boundary. From L4 to L9, the peak value increased and its location moved farther away from the top. The potential for erosion of the under surface of the jam was higher at L8 and L9 (near the toe of the jam) due to the high turbulence intensity in this upper area. The high turbulence intensity near the ice cover would increase turbulent mixing and heat transfer which could promote melting of the underside of the cover, thereby decreasing the jam roughness. In this region, the overall average of the turbulence intensity is less than the EQR due to the flow acceleration. Although the near-bed velocities and bed shear stresses have been both shown to increase near the jam toe – thereby promoting bed erosion - the average streamwise turbulence intensities in this region are actually less than in the EQR.

In the LTR (Fig.9 (d)), the peak value at L10 was much larger than the peak value at L9 and it moved farther from the upper boundary in comparison with L9. Thus, there could be a greater potential for surface erosion in this area compared to L8 and L9. As the flow developed in this region, the peak value moved towards the upper boundary due to the decelerating and expanding flow.

In the DIS (Fig.9 (e)), the effect of the upper boundary on the turbulence intensity distribution decreased as far as it changed to resemble that of the EQR upstream. The average of the turbulence intensity in this region is higher than the downstream transition.

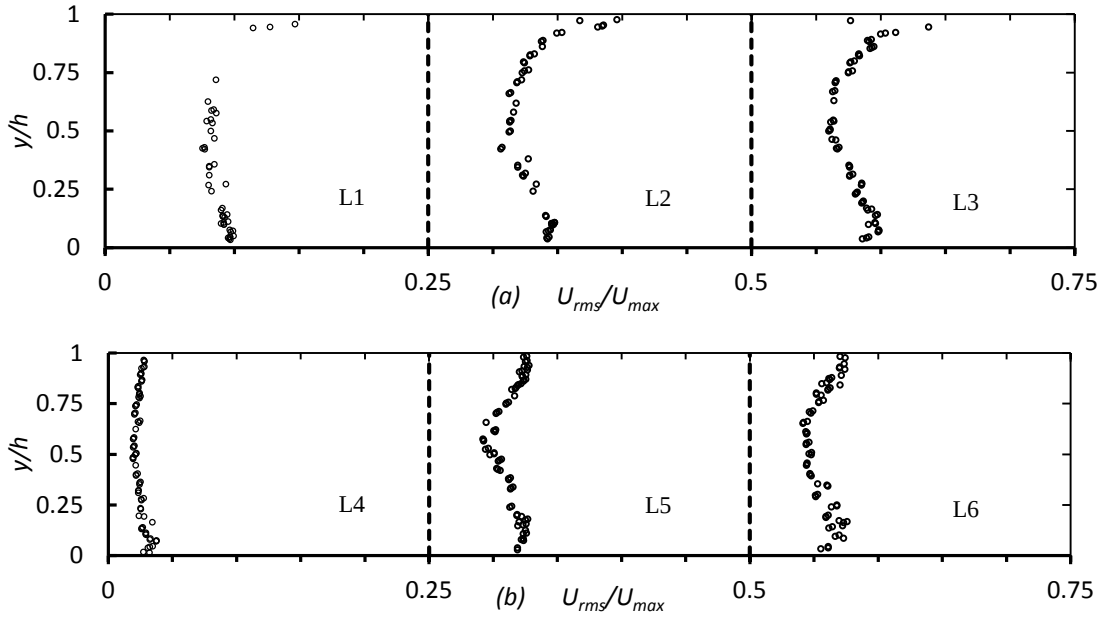

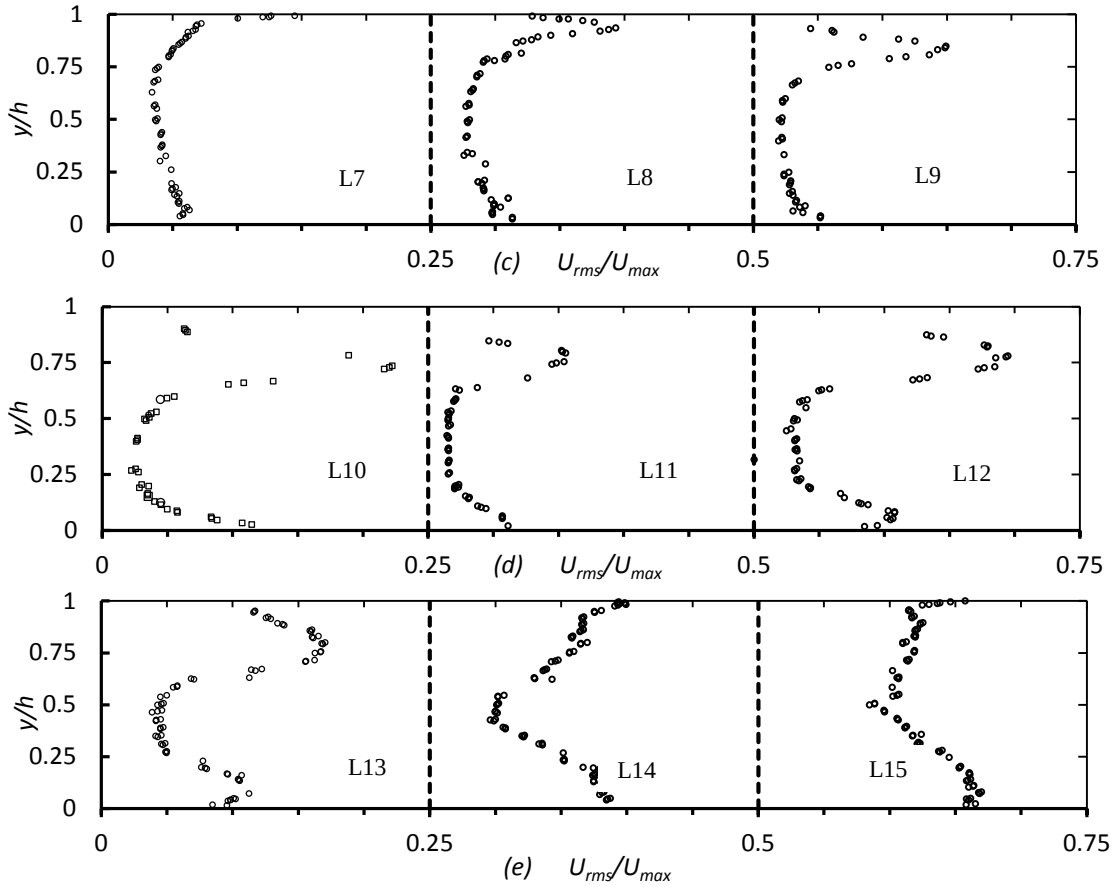

Figure 9. Dimensionless streamwise turbulence intensity in the (a) EQR, (b) and (c) UTR, (d) LTR, (e) DSI

5. Conclusions

An experimental study was conducted in the Hydraulic Research and Testing Facility at the University of Manitoba to examine the effect of an ice jam on the streamwise velocity distribution and streamwise turbulence intensities. Velocity measurements were taken in the fully developed region over a smooth bed and under a smooth ice jam, at various locations along the water column in the centerline of the channel using an ADV. The measurements indicated the streamwise velocity distribution and turbulence intensities are a function of position underneath an ice jam. The maximum velocity beneath the entire ice jam measured in this experiment occurred near the toe of the jam in the UTR. At this position, the location of the maximum velocity is closer to the channel bed than the cover, which generates a higher bed shear stress that has the potential to increase the risk of scour. The streamwise turbulence intensity is smallest near the mid flow depth and increases towards the bed and ice jam surface. The total pattern of the turbulence intensity profiles in the EQR were similar to the findings of Parthasarathy & Muste (1994) and Robert & Tran (2012). The maximum turbulence intensity was observed near the toe of the jam, close to the cover. The higher turbulence intensity in this region can influence the ice jam evolution by promoting turbulent mixing that will increase heat transfer. This will erode the under-side of the ice cover and decrease the ice roughness. Knowledge of the velocity and turbulence intensity beneath an ice jam may also shed light on the potential for erosion or deposition of entire ice blocks from within the jam or travelling within the flow.

For future work, the vertical component of velocity, shear stresses and turbulent flow quantities such as the Reynolds shear stresses and vertical turbulence will be analysed. In addition, the turbulent flow features beneath a simulated rough ice jam should be investigated.

6. Acknowledgments

This research was funded the Natural Sciences and Engineering Research Council of Canada and Manitoba Hydro. The authors kindly acknowledge Dr. Karen Dow, Lucas Wazney, Alexander Wall, Mitchel Peters, and Bethany Heppner for their contributions.

7. References

Beltaos, S., Moody, W.J., 1986. Measurements of the configuration of a breakup jam. Hydraulics Division, National Water Research Institute, Canada Centre for Inland Waters, Burlington, Canada, 1-15.

Beltaos, S., Burrell, B., Ismail, S., 1996. 1991 ice jamming along the Saint John River: a case study. Canadian Journal of Civil Engineering, 381-394.

Beltaos, S., 1993. Numerical computation of river ice jams. Canadian Journal of Civil Engineering, 88-99.

Beltaos, S., 1995. River ice jams. Water Resources Publication.

Beltaos, S., Burrell, B.C., 2002. Extreme ice jam floods along the Saint John River, New Brunswick, Canada. Proceedings of a symposium held at Reykjavik, iceland, Wallingford, UK, 9-14.

Beltaos, S., 2008. River ice breakup. Water Resources Publication.

Carson, R., Beltaos, S., Groeneveld, J., Healy, D., She, Y., Malenchak, J., Morris, M., Saucet, J.P., Kolerski, T., Shen, H.T., 2011. Comparative testing of numerical models of river ice jams. Canadian journal of civil engineering, 669-678.

Healy, D., Hicks, F., Loewen, M., 2002. Unsteady velocity profiles under a floating cover. Proceedings of the 16th IAHR international symposium on ice, Dunedin, New Zealand, 111-118.

Hicks, F.E., Bonneville, C., 1998. Modelling ice jam evolution processes. Ice in surface waters, Balkema, Rotterdam, 93-99.

Kowalczyk, T., Hicks, F., 2003. Observations of dynamic ice jam release on the Athabasca River at Fort McMurray, AB. Proceedings of 12th Workshop on River Ice, Edmonton.

Nortek, 2013. Comprehensive Manual for acoustic Doppler velocimeter.

Parthasarathy, R.N., Muste, M., 1994. Velocity measurements in asymmetric turbulent channel flows. Journal of hydraulic engineering,American Society of Civil Engineers, 1000-1020.

Pariset, E., Hausser, R., 1961. Formation and evolution of ice covers on rivers. 41-49.

Prowse, T.D., 1986. Ice jam characteristics, Liard-Mackenzie rivers confluence. Canadian journal of civil engineering, 653-665.

Robert, A., Tran, T., 2012. Mean and turbulent flow fields in a simulated ice-covered channel with a gravel bed: some laboratory observations. Earth surface processes and landforms, Vol. 37, 951-956.

Shen, T., 2002. Development of a comprehensive river ice simulation system. Proceedings of the 16th IAHR international symposium on ice, Dunedin, New Zealand, 142-148.

She, Y., Andrishak, R., Hicks, F., Morse, B., Stander, E., Krath, Keller, D., Abarca, N., Nolin, S., Tanekou, F.N., Mahabir, C., 2009. Athabasca River ice jam formation and release events in 2006 and 2007. Cold Regions Science and Technology, 55(2), 249-261

Wuebben, J.L., 1988. A Preliminary study of scour under an ice jam. Proceedings, 5th workshop on hydraulics of river ice/ice jams, Winnipeg, Canada, 177-189.

Yamaguchi, H., Hirayama, K.I., 1990. Measurements of flow velocity under the ice cover. IAHR ice symposium, Espoo, 1155-1170.

Zulfet, E., Ettema, R., 1997. Unsteady ice jam processes. CRREL Rep. 97-7, U.S. Army cold regions research and engineering laboratory, Hanover, N.H.